HEWLETT-PACKARD JOURNAL

Cover: **LARGE-SCREEN ELECTROSTATIC CRT FOR 20 MHz DISPLAY; pages 2 and 10**

See Also: **1967 FLYING CLOCK EXPERIMENT; page 12**
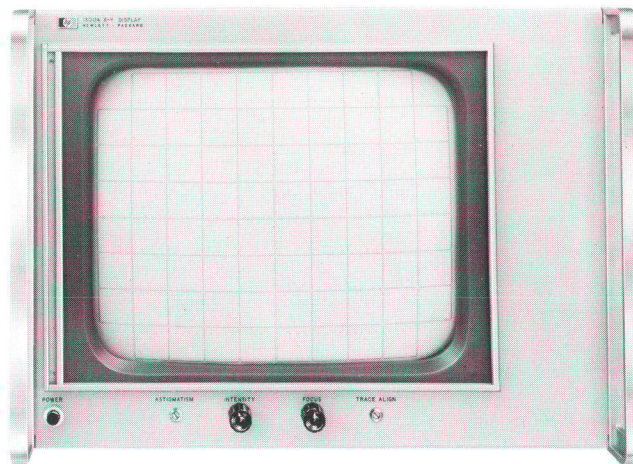
Large-Screen High-Frequency X-Y-Z Display

Expanded-mesh CRT's (see page 10) have made possible a bright 8 by 10 inch display with bandwidths greater than 20 MHz

By Charles House

Fig. 1. *Wide bandwidth of 20 MHz on an 8 x 10 inch CRT display is provided by the HP Model 1300A X-Y Display. All solid state, the instrument uses a CRT designed to give a bright display with high sensitivity.*

LARGE-SCREEN CATHODE-RAY TUBE DISPLAYS are invaluable for presentation of computer data, classroom displays, medical monitoring, or production line analysis. Both magnetic and electrostatic CRT units are presently used in these applications, but each has unique problems which limit its desirability. Many applications using small-screen oscilloscopes are areas where a larger screen would be more desirable if costs and performance were compatible.

Of the two types of large-screen displays, the magnetic CRT is cheaper, offers better resolution, and is an easier tube for deflection amplifiers to drive at low speeds. However, to attain X and Y bandwidths greater than about 20 kHz, the deflection amplifiers become relatively expensive; to achieve even 1 MHz bandwidth becomes a nearly prohibitive task. Television receivers and monitors are typically 5 MHz bandwidth on the z-axis only. Additionally, to achieve good linearity in magnetic systems,

either high-quality deflection yokes or a feedback-linearizing circuit must be employed.

Thus at higher speeds, the electrostatic tube has the advantage because of the very sophisticated amplifiers required with a magnetic tube. The electrostatic tube, however, is usually very long, with quite insensitive deflection plates. A typical 8 by 10 inch display tube is about 30 inches long with deflection factors of 75 to 100 volts per inch. The deflection amplifiers are generally transmitter tube designs which require high power, fan cooling, and frequent service.

Another approach directed toward fast computer readout is a combination CRT, which employs magnetic deflection for movements larger than one inch, and electrostatic deflection for smaller movements. This allows writing many characters in a one inch square very rapidly, and then going slowly to the next square, to repeat the fast sequence. Many more characters may be written this way than with a conventional magnetic display unit; yet only a small electrostatic deflection amplifier is required and the CRT need not be very long. Cost of such a CRT is relatively high.

A new electrostatic CRT development has been incorporated into an instrument which overcomes a num-

ber of limitations found in traditional large-screen displays. The HP Model 1300A X-Y Display, Fig. 1, offers the speed and linearity associated with quality electrostatic units, and in addition achieves the reasonable size, weight, and cost usually found only in magnetic deflection CRT's.

The cathode ray tube is a result of combining an electrostatic gun using a high-expansion contour mesh[1] with a short, wide-scan bottle. The CRT is less than 18 inches long with greater than 8×10 inch display area because of the expansion afforded by the contour mesh. The expansion also improves the CRT deflection factor to 13.5 volts/inch for both x and y axes. This allows completely solid-state circuitry in the display unit.

Several large-screen applications require a high-quality z-axis amplifier. A direct-coupled wide-band analog amplifier is provided with this display unit, with optional preset gray-scale digital inputs. Additionally, a digital blanking input is provided for oscilloscope applications. The X and Y deflection systems are identical, resulting, among other things, in identical phase shift to quite high frequencies.

The Model 1300A offers 1-volt full-screen deflection inputs on the X and Y amplifiers, which makes it compatible with most sources capable of driving an X-Y recorder. The z-axis analog input requires $+1$ volt to go

from full intensity to full 'OFF', giving a sensitive control point for high-speed z-axis signals. All of the above inputs have vernier attenuators for greater than 2.5:1 reduction in sensitivity.

Z-Axis Amplifier

Rapid beam intensity modulation is required to realize the full potential of a high speed X-Y display for character or pattern generation. The Model 1300A accomplishes this with a direct-coupled, 20 MHz, analog input, z-axis amplifier.

Z-axis amplifiers for CRT displays often have one of two major limitations for character-writing. Bandwidth is an indication of how fast a dot may be intensified and turned off, and is clearly of importance to high speed character or format generation. Phase shift or time delay between z-axis and x-y axes is of great importance if random-access positioning and intensifying of characters are to occur in the proper sequence.

A bandwidth specification measured by a continuous wave response, defining bandwidth as the frequency where the gain is 3 dB down from the mid-band gain, is required to define clearly the z-axis speed capability for character generation. A common 'specification' is a bandwidth derived from the pulse response rise time, which neglects to mention either fall time restraints or amplifier saturation time delays. These often reduce the true CW bandwidth to the point that alphanumeric information is impossible to portray at the desired speed. The Model

[1] Floyd G. Siegel, 'A New DC-50+ MHz Transistorized Oscilloscope of Basic Instrumentation Character,' **Hewlett-Packard Journal,**' Vol. 17, No. 12, August 1966.
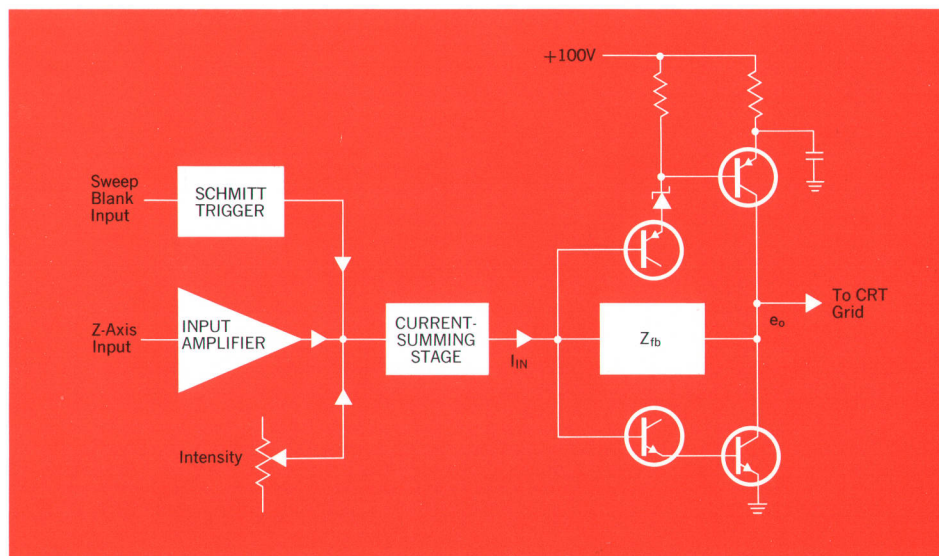

Fig. 2. *The Model 1300A z-axis amplifier is direct coupled. I_{in} is the sum of currents from three sources, shown.*

1300A z-axis input is truly 20 MHz measured with the continuous sinusoidal wave technique; additionally pulse rise time (10% to 90% points) is measured and specified less than 20 nanoseconds.

Phase shift between the X and Y amplifiers is specified less than 0.1 degree to 50 kHz and less than 1 degree to 1 MHz. There is approximately a 7 nanosecond time lag between the z-axis control of the CRT beam and the X and Y control of the beam. This accounts for a typical phase shift of approximately 1 degree at 1 MHz, growing to 10 degrees at 20 MHz, between the z-axis input and inputs to the X and Y amplifiers.

A 50 volt signal is necessary at the CRT grid in order to go from a blanked condition to full intensity. To be able to swing 50 volts in 20 nanoseconds, the amplifier must be able to supply peak currents of over 60 mA to charge the tube and stray capacitance. In a conventional class A amplifier such as those of the X and Y systems, the bias current should be at least 60 mA which results in high power dissipation.

Output Stage

The Model 1300A gate amplifier utilizes a complementary output stage in which the bias current through either output transistor needs only to be equal to the average current through the transistor and not the peak current.

The principal difference between the Model 1300A amplifier and other complementary output amplifiers is that this circuit uses direct coupling to both output transistors, Fig. 2. If capacitive coupling is used to one or both tran-
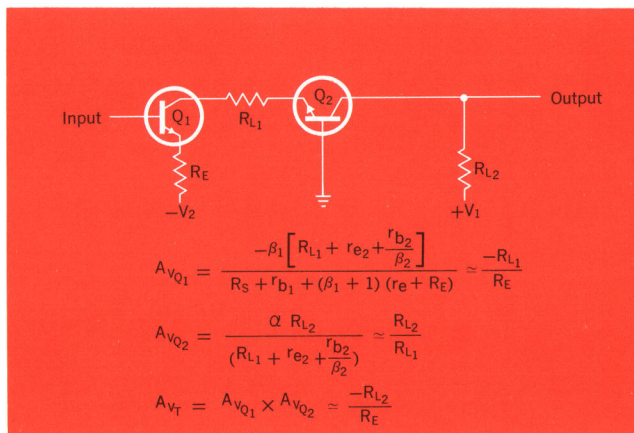
Fig. 4. *A base-feedback cascode circuit used in the X and Y deflection amplifiers permits relatively low-voltage, high-speed devices to achieve necessary dynamic range and fast deflection.*

$$A_{V_T} \simeq \frac{-R_L \| (R_A + R_B)}{R_E}$$

sistors, a condition may exist at high repetition rates in which the base current requirements are greater than the average current through the bias network and the amplifier ceases to function properly. This direct coupling is what permits the Model 1300A gate amplifier to reproduce 20 MHz sinusoidal signals.

The output stage is operated as an operational amplifier in which a current source replaces the input impedance giving an output e_o, equal to $-Z_{fb}I_{in}$. The input current, I_{in}, is the sum of currents from three sources — the intensity control, the linear input amplifier, and the digital sweep blanking circuit.

The linear input requires $+1$ volt to fully blank the display from maximum intensity, or -1 volt to fully intensify from a blanked condition. Any intermediate intensity is available with the appropriate input voltage. A gray-scale, or sequential series of intensity shadings, may be defined for as many as eight levels if desired. The linear input has a 2.5:1 vernier to provide reduction in gain. Additionally, a balance control is available to allow nulling of input dc-level offsets of ±1 volt.

The sweep blanking input allows digital control of the beam by blanking the display as the input is raised from -3 volts to ground. This may be done by contact-closure to ground of less than 1000 ohms; an 'open-circuit' impedance of greater than 20 k ohms will allow full intensity. This input may typically be cycled at rates to 1 MHz.

One other beam control is provided — the chop blanking input, which is useful when multiple traces are displayed by means of an electronic switch. A $+50$ volt pulse is required for blanking on this ac-coupled input. This input is open-circuited and the internal lead is grounded by a rear-panel switch when not in use.

$$A_{V_{Q_1}} = \frac{-\beta_1 \left[R_{L_1} + r_{e_2} + \frac{r_{b_2}}{\beta_2} \right]}{R_S + r_{b_1} + (\beta_1 + 1)(r_e + R_E)} \simeq \frac{-R_{L_1}}{R_E}$$

$$A_{V_{Q_2}} = \frac{\alpha\, R_{L_2}}{(R_{L_1} + r_{e_2} + \frac{r_{b_2}}{\beta_2})} \simeq \frac{R_{L_2}}{R_{L_1}}$$

$$A_{V_T} = A_{V_{Q_1}} \times A_{V_{Q_2}} \simeq \frac{-R_{L_2}}{R_E}$$

Fig. 3. *Transistorized equivalent of the cascode amplifier. $A_{V_{Q_1}}$ and $A_{V_{Q_2}}$ are the voltage gains of transistors Q_1 and Q_2; A_{V_T} is the total amplifier gain; β_1 and β_2 are the beta current gains of the transistors, r_e and r_b are resistances of the emitter and base respectively; R_s is the source resistance of the generator driving the amplifier.*
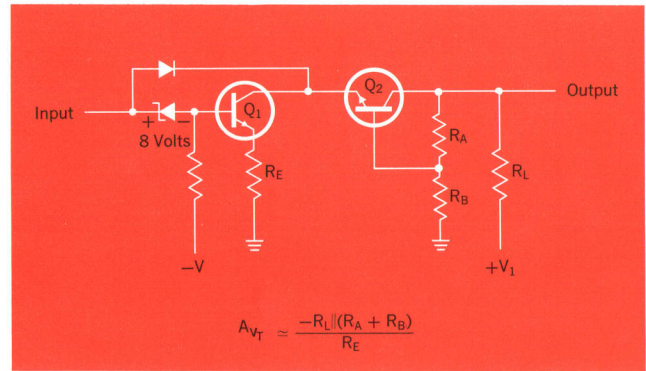
4

Repeatability and Settling Time

Two parameters of vital concern to many display systems are repeatability and settling time. Repeatability is a measure of the ability to hit the same spot again from any point on screen, and may be thought of as repeatable accuracy to a given X-Y co-ordinate. Settling time is considered to be the total time required for deflecting the beam from one position to another within a stated accuracy, which means that it is the step function response time to within some small percent of final value.

Terminology changes with different manufacturers on these parameters. Other names for repeatability include: plotting accuracy; line relocation accuracy; and random access accuracy. Settling time is also referred to as: step function response; random positioning time; beam deflection time; random positioning, traverse, and settling time; beam slewing and settling time; and jump-scan time

To illustrate a way in which random access repeatability errors affect a display, consider the CRT display sketched in (a). This display is a portion of a production test sequence, where the signal displays and grid co-ordinates change periodically.

For such displays, the characters and grid are computer-generated and multiplexed with the signal displays at a rate just above CRT phosphor flicker. The X and Y amplifiers may be at any position on screen when commanded to re-write the grid and characters.
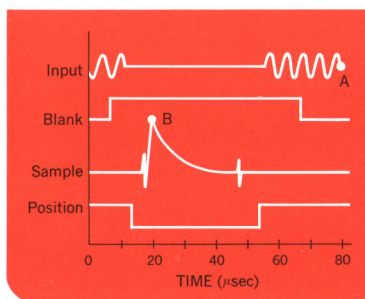
Assume for the first drawing of the grid that the beam was already at the 0,0 co-ordinate of the grid. For the first re-tracing of the grid, the beam was at point A tracing the signal display when commanded to return to the 0, 0 co-ordinate. For the second re-tracing, the beam was at point B. In (b), are shown the beam deflection vectors which the amplifiers must follow (while the beam is blanked) in order to retrace the grid.

If the repeatability error of the amplifiers is 1% for all three cases, it can be seen that 1% of zero deflection
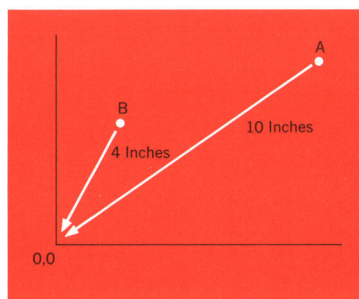
when the grid was first written was zero error, while for point A, the error is 0.1 inch, and for point B, the error is 0.04 inch. The grid origin detail shown in (c) shows the grid jitter created by two such re-tracings. Character generation and refresh will suffer from the same problem. Repeatability should be within one-quarter to one-half trace width for a full-screen deflection relocation to avoid objectionable trace thickening.

Two of the most troublesome problems facing the designer seeking to eliminate repeatability error are non-linear input capacitances and thermal time-constants within the amplifier. Important to the success of the Model 1300A amplifer design in meeting the repeatability specification of 0.15% maximum error were the decisions first to eliminate attenuators from both the X and Y inputs, and second, to use differential amplifiers from input to output in both amplifiers. Careful attention to dielectric materials and lead routing has minimized the frequency-dependent non-linearities in the input circuit. Repeatability and settling time specifications are valid only without high impedance attenuators at the inputs.
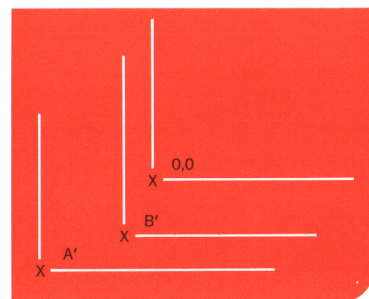
Thermal time-constants are particularly troublesome for solid-state designs. Changes in bias level with signal inputs cause changes in heat dissipation, and very frequently in performance characteristics such as transistor V_{be} or beta. A common way to avoid thermal time-constant problems is to employ differential amplifiers, so that thermal time-constants will be developed equally in both halves of the amplifier with the bias changes caused by an input signal. Thus, the time-constants become common-mode signals which are rejected by the amplifying action of the differential amplifier. The Model 1300A X and Y amplifiers are differential throughout, with an additional bias adjustment at the first gain stage to adjust for power tracking, in order to optimize the repeatability performance of the display.

(a)

(b)

(c)

X-Y Deflection Amplifiers

Deflection systems for cathode ray tubes have a number of restrictive design parameters. In most electrostatic large-screen display units, the high voltage drive requirements have been met with transmitter tube designs. One recent solid-state system employed series-parallel combinations of 500-volt transistors in order to obtain adequate dynamic range. The Model 1300A CRT eases the deflection requirements on dynamic range, but the combination of dynamic range and bandwidth achieved required careful circuit design.

Cascode amplifiers were originally developed with tube techniques; a transistorized equivalent is shown in Fig. 3. They possess a number of advantages over other forms of cascaded pairs of active devices.

One advantage is that the overall gain function is seen to be independent of R_{L_1}. At higher frequencies this is not strictly true because of the Miller capacitance affecting the total circuit input impedance, but even then, it is found that R_{L_1} offers a point where signal control may be accomplished with a minimum of undesired effect on the broadband characteristics of the circuit or the signal. Thus the cascode in this form is often used with channel switching, gain and balance control, or sync signal derivation being done in the R_{L_1} locale.

Another major advantage is that the second transistor is being operated as a common-base amplifier, which allows use of the BV_{CBO} rating rather than the lower BV_{CEO}. Since this will be the transistor driving the CRT in an output cascode, more dynamic range for a given transistor type is thus achievable. The transistor is only being used for alpha gain rather than beta gain, which allows higher bandwidth from this stage than if the same device were operated as a common-emitter amplifier.

If the cascode is differential, a high degree of common-mode rejection may be attained for input signals or for thermal time-constants developed by large power changes with signal in the transistors. In an output stage with large signal swings, this is important to avoid repeatability error. The thermal time-constants are best rejected if the amplifier is 'power-matched', which entails matching the maximum power of Q_1 to the power in R_{L_1} at that bias, and also matching the maximum power of Q_2 to the concurrent power in R_{L_2}. Note that since each device is power-matched to its own load, quite different devices in terms of thermal time-constants (governed by chip geometry and header construction) may be used for Q_1 and Q_2. Because of the Miller effect on Q_1, this device is often chosen for high f_t and low $r_b' C_c$, rather than V_{ceo} and power dissipation. Conversely, Q_2 is chosen primarily for power dissipation, BV_{CBO}, and C_{ob}.

For the Model 1300A CRT deflection system, the cascode's last two advantages appeared particularly valuable. A figure of merit for a high-speed deflection device on an electrostatic tube may be described as output capacitance/power dissipation capability. Since the dynamic range is specified by the CRT voltage deflection requirements as some V_{total}, and speed of deflection is often limited by the current-charging capability of the amplifier into the total output capacitance of the transistor, CRT plates, and stray, it can be seen that maximum power of the output device is directly related to the achievable deflection speed.

For such a case, a slight modification of the cascode circuit, Fig. 4, is of value. Note that the base of the output transistor Q_2 is now controlled by feedback from the output signal. This allows shift of some of the total dynamic range requirement back to Q_1. In the balanced situation, the dynamic range will be equally shared by the two devices. This allows using a lower breakdown voltage device and higher current to charge the output capacitance for a given power dissipation per device.

The base-feedback cascode has other advantages over the conventional cascode for some deflection requirements. Note that C_{cb} of the output transistor is now reduced by the feedback ratio, which enhances the figure of merit discussed above. Additionally, the power-matching requirement to null out thermal time-constants now requires only that the combined power dissipation of Q_1 and Q_2 at maximum power equal the concurrent
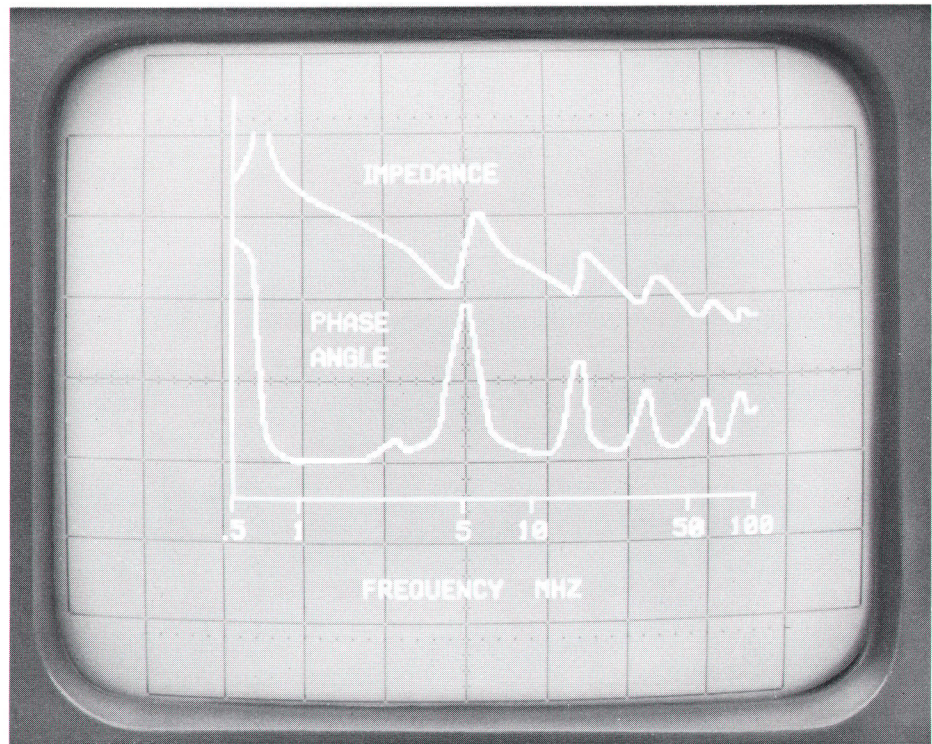
Charles House

Chuck House joined Hewlett-Packard in 1962 as a development engineer. He worked on several plug-ins for the HP Model 140A Oscilloscope and later worked on the design of the HP Model 155A Programmable Oscilloscope. He is presently project leader in the low-frequency oscilloscope development laboratory.

Chuck received his BS degree in solid state physics in 1962 from the California Institute of Technology. In 1964 he earned his MSEE from Stanford University on the HP Honors Cooperative Program. He is presently attending the University of Colorado working on an MA degree in History of Science.

Fig. 5. *Alphanumeric displays, in conjunction with graphic presentations, are finding increasing use throughout the computer readout field. The display shows the high frequency parameters of an inductor, and is fed to the X-Y monitor from the HP Model 2116A Computer.*

power of R_L. This presumes that Q_1 and Q_2 are now the same device in terms of thermal time-constants, which is not unreasonable since both require the same power dissipation and V_{ceo} to realize the benefit of sharing the dynamic range.

The use of the base-feedback cascode in both the X and Y deflection amplifiers has allowed using relatively low voltage, high speed devices to achieve adequate dynamic range and quite fast deflection. The transistors used are TO-5 case silicon devices with very low C_{ob} and high f_t. The use of beryllium oxide heat conductors to the finned heat sinks has allowed device operation at maximum power of 1.75 watts to ambient temperatures beyond 55°C. Typical performance of the vertical system is in excess of 25 MHz for an 8 inch reference, while the horizontal is approximately 22 MHz. The difference is due to the different plate capacitances of the CRT.

One other circuit feature of interest is the use of anti-saturation diodes at the input of the base-feedback cascode. The dynamic range of the output cascode is about 13 inches total deflection (± 6.5 inches from center screen), which is adequate for any on-screen display.

One intent of the settling time specification, and indeed of the wide dynamic range of the input (in excess of ± 50 inches), is to allow large off-screen deflections and returns to within 0.25% of final value within 200

nanoseconds. This is particularly useful for relative time studies of two or more signals with small high-frequency perturbations on top of large signals. The problem which may arise without the output anti-saturation circuit is that the output transistors have a saturation storage time as long as 700 nanoseconds, which allows gross errors in high-speed time studies.

The diodes hold a minimum of 8 volts across Q_1 with overdrive conditions of up to ten screen diameters; the resistance loads are such that Q_2 is similarly quite far from forward bias of the collector-base junction under such conditions. This allows faithful time correlation of large overdrive signals at rates up to 20 MHz, and in reality extends the settling time specification to include signals as large as ± 50 inches from center screen.

Computer Readout Displays

Magnetic CRT displays are ordinarily used in digital computer readout consoles because of spot resolution and cost considerations. As higher clock-rate speeds are used, magnetic displays often become display-limited because of the relatively slow beam slew rate or X-Y deflection rate of the magnetic CRT and amplifiers. The electrostatic tube in the Model 1300A offers much more speed for random access printout formats, which the modern high-speed computers are capable of producing. Fig. 5 shows a typical digital computer graphic display.
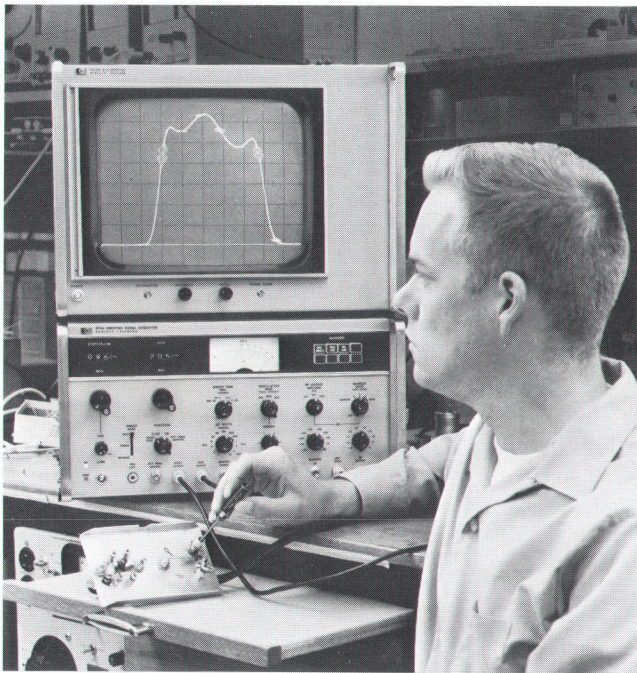
7

Fig. 6. *Spurious signals are easily seen on swept-frequency displays with the wide-band capabilities of the Model 1300A. This sweep display is provided by the HP Model 675A 10 kHz to 32 MHz Sweep Oscillator.*
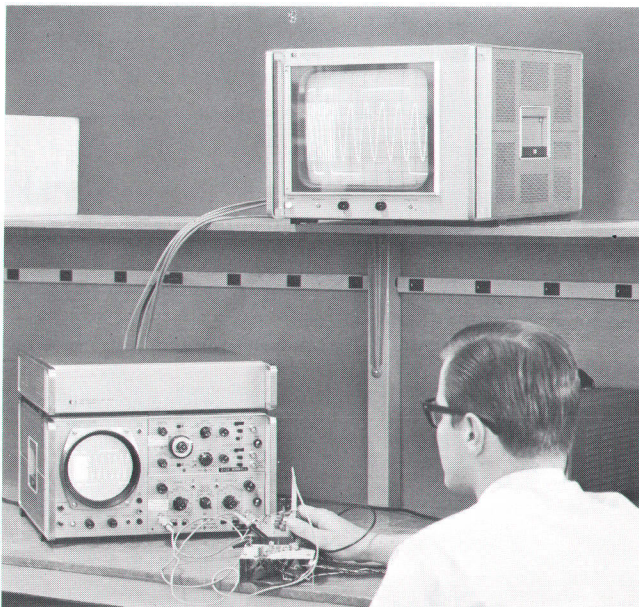

Fig. 7. *High-frequency oscilloscope displays for classroom or production-line are possible on the large-screen presentation. Shown is a mating box for the HP Model 140/141A Oscilloscopes to allow remote displays on the Model 1300A.*

The analog and hybrid computer readout requirements are somewhat different, for the typical presentation is a multiplexed set of signals from different amplifier outputs which are displayed as graphs of related information. The requirement on resolution is often not as stringent as for the high-quality digital display, but the X and Y deflection rate requirement is much more severe. Multiplexing often demands switching rates beyond 20 kHz, which entails beam deflection rates equivalent to 1 MHz bandwidths and higher. These applications very often require Z-axis speeds in excess of 5 MHz as well, in order to achieve the blanking requirements for the multiplexed display. The Model 1300A is able to achieve 20 MHz bandwidths on all three axes for full-screen deflection, which more than adequately meets the needs of analog computer display requirements.

Of the pertinent parameters of analog computer displays, perhaps none are more important than settling time and repeatability. These parameters in large measure determine the quality of the display for high speed multiplexing of signals. The Model 1300A has been designed to achieve high levels of repeatability (0.15% repeatability error) and quite fast settling time (less than 200 nanoseconds to within a trace width of final value).

Swept Frequency Plotting

Because the display is large and easily read, and because the wide-band capability allows high-frequency spurious signal observation, the Model 1300A is ideal for examining the response characteristics of filters and amplifiers, Fig. 6. The wide-band X and Y amplifier response is of importance to many such applications where high-frequency spurious signals are transmitted from the oscillator or are generated in the network under test. Conventional large-screen magnetic displays cannot display such information, which is valuable not only to the engineering analysis, but frequently critical on the production line.

Classroom Displays

Large-screen displays have been used in classroom applications for a number of years; their size and easy readability from a distance being prime assets for a number of people trying to see a demonstration. Most classroom monitors are TV-monitor units, with magnetic tubes which use raster displays. Seminar presentations and laboratory demonstrations, as well as many classroom presentations, often would like to present oscilloscope-type displays of higher-frequency phenomena than the typical classroom monitor permits. The small size of the Model 1300A package in relation to display area,

combined with the bright trace and wide-band capability, enables a substantial improvement in teaching displays.

Production Line Displays

Large-screen oscilloscopes have appeal for many production-line uses, where easier resolution offers less fatiguing viewing for the operator who must resolve oscilloscope displays all day. Although most production lines do not require extremely wide bandwidths for oscilloscopes, the general need is for displays capable of 100 kHz to 10 MHz rather than the 20 kHz capability of present large-screen magnetic displays.

The Model 1300A may be deflected by any oscilloscope having X and Y outputs to drive recorders. A z-axis or blanking signal output is necessary for the optimum display. The HP Model 155A/1550A Programmable Oscilloscope and the sampling plug-ins for the HP Models 140A/141A Oscilloscopes are capable of driving the 1300A with only a minor Z-axis modification.

For true oscilloscope versatility, a plug-in capability for vertical and horizontal systems is the most flexible approach.[2, 3] Fig. 7 illustrates one such system.

Acknowledgments

Electrical design of the HP Model 1300A X-Y Display was by Thomas K. Bohley, Alan J. DeVilbiss, and the undersigned; product design was by Thomas Schroath; industrial design was by Andi Aré, and technician support by Robert K. McCullough. Milton E. Russell was responsible for the cathode ray tube development. John H. Strathman, Engineering Manager of the Low Frequency and Special Projects laboratories, contributed substantially to the project development with much appreciated encouragement and valuable suggestions. *hp*

Fig. 8. *Used in a system such as the HP Model 8540 Automatic Network Analyzer, the Model 1300A X-Y Monitor provides a large, easy-to-read display.*

[2] Richard E. Monnier, 'A Basic New Wide-Band Oscilloscope with Planned Anti-Obsolescence,' '**Hewlett-Packard Journal,**' Vol. 15, No. 1, September 1963.

[3] Floyd G. Siegel, 'A New DC-50+ MHz Transistorized Oscilloscope of Basic Instrumentation Character,' **Hewlett-Packard Journal,** Vol. 17, No. 12, August 1966.

Factors in Designing a Large-Screen, Wideband CRT

By Milton E. Russell

THE LARGE-SCREEN DISPLAY FIELD has been dominated by magnetic-deflection CRT systems. This has been due in part to certain disadvantages of conventional electrostatic-deflection tubes, primarily the very high deflection voltage required and long tube length required for a large display. Because of the demands of the TV industry great strides have been made in deflection yoke design and in wide-angle magnetic-deflection CRT design. Deflection angles have increased from about 50 degrees in the early days of television to the 110 to 114 degree designs common today. In computer and TV monitor displays, where greater precision and minimum defocusing are necessary, 70 to 90 degrees deflection angles are more common. The magnetic tube, if properly designed, has the advantages of small spot size, high brightness, and low cost. But where broad bandwidth (above about 1 MHz) is desired, the electrostatic tube is necessary.

Most large-screen electrostatic-deflection tubes are of the conventional post-accelerator design. In this design, the shape of the post-acceleration field tends to reduce display size. The reduction becomes greater as post-acceleration ratio (ratio of screen voltage to gun voltage)

A very large CRT display in a relatively short envelope (Model 1300A CRT, left) can be obtained by suitable design of the expansion mesh. Other engineering factors appropriate to specific applications may dictate an expansion mesh design to accommodate smaller displays.

is increased. Screen voltage must be high for adequate brightness, therefore gun voltage must be high, with poor deflection sensitivity as a consequence. Center screen spot size is typically small, but the large deflection angles required to keep tube length within reason cause considerable deflection defocusing. Dynamic correction voltages are commonly applied to reduce defocusing.

Typical electrostatic deflection tubes, comparable in display size with the new Model 1300A CRT, are on the order of 23 inches long, with deflection factors of about 100V/inch and center spot size of about 14 mils.

With the advent of expansion mesh tube development, the electrostatic deflection approach overcomes some of its previous shortcomings. It can easily be driven with solid state circuitry and has entered the length domain of magnetic deflection tubes. Performance achievable by using expansion meshes has been incorporated in several HP scope systems. Since first introduced in the HP Model 175A Oscilloscope, mesh tubes have been designed to meet the particular needs of other HP oscilloscope systems.[1,2,3,4] This experience has helped to make rather dramatic extensions of the art in the design of the cathode ray tube for the HP Model 1300A X-Y Monitor. Its display is 8×10 inches, with a 13.5 V/inch deflection factor, a length of 17¾ inches, and a center spot size less than 20 mils.

Deflecting angles in the deflection plate region must be small to achieve high sensitivity with minimum deflection defocusing. The mono-accelerator equivalent model (see sketch) is the way the tube would look if no post deflection acceleration were used. The deflection angle is low. The required tube length for the 8×10 inch display would be 42 inches.

By adding the contoured high expansion mesh operating at gun potential, and a separated conductive coating on the bulb wall operating at higher potential, a strong field is formed between mesh and bulb wall with large radial as well as axial components. The beam is acted upon by forces in both axial, F_A, and radial, F_R, directions resulting in acceleration and expansion of the beam. Field shape is critical, and is controlled by the contour of the mesh in combination with the boundary shape of the bulb wall. Vertical expansion of the display $\left(\dfrac{D'}{D}\right)$

[1] Floyd G. Siegel, 'A New 50 MC Oscilloscope Based on an Advanced CRT Design,' **'Hewlett-Packard Journal,'** Vol. 13, No. 8, April 1962.

[2] Richard E. Monnier and Ralph R. Reiser, 'A New TV Waveform Oscilloscope for Precision Measurements of Video Test Signals,' **'Hewlett-Packard Journal,'** Vol. 17, No. 6, Feb. 1966.

[3] Floyd G. Siegel, 'A New DC-50 MHz Transistorized Oscilloscope of Basic Instrumentation Character,' **'Hewlett-Packard Journal,'** Vol. 17, No. 12, August 1966.

[4] Richard E. Monnier, 'A Basic New Wideband Oscilloscope with Planned Anti-Obsolescence,' **'Hewlett-Packard Journal,'** Vol. 15, No. 1, Sept., 1963.

Use of the expansion mesh post-accelerator reduces tube length for an 8 by 10-inch display to about 17¾ inches (a). An equivalent mono-accelerator tube without the expansion mesh (b) would require an envelope nearly three times as long.

is 3.3 × vertically, and 2.7 × horizontally (area expansion 9 ×). This results in compression of actual tube length from 42 inches down to 17¾ inches. The tube is then relatively short in actual physical length, but appears long to the deflection plates.

Spot size is another important consideration. Several factors contribute to spot size growth. One of these is the magnification ratio, $\frac{Q}{P}$, the ratio of distance from lens to screen, to the distance from 'crossover' to lens. (The crossover is the point of minimum beam cross section and is located near the control grid aperture.) Spot size is proportional to $\frac{Q}{P}$. In the Model 1300A CRT, Q is the same as the monoaccelerator equivalent, and so is long because of the low deflection angle. To compensate, a relatively long gun and consequently long P distance was chosen.

Another consideration is spot growth due to space charge repulsion. Space-charge spot growth is a direct function of distance from lens to screen and an inverse function of beam voltage. The Model 1300A CRT has a relatively short path length from lens to screen and beam velocity is high for a considerable portion of that distance. Consequently, space-charge spot growth is not significant.

The mesh intercepts about half of the beam current, requiring higher gun currents to produce equivalent amounts of screen current. High screen voltage (20 kV) is used to compensate. Also, the mesh openings produce aperture lenslets which tend to defocus the beam, the effect increasing as opening size increases. The mesh then acts as a resolution limiting element similar to grain structure in a phosphor screen. Very fine mesh is used on the Model 1300A tube, resulting in a limiting spot size, due to mesh aperture effects alone, of about 8 mils.

The net effect of all the contributors to spot growth is a spot size of 20 mils or less at center screen at 100 foot-lamberts brightness (shrinking raster method) with maximum edge spot size of 30 mils.

Acknowledgments

Milton E. Russell

Milton Russell graduated from the University of Connecticut in 1951 with the degree of Bachelor of Science in Electrical Engineering. Previous to joining Hewlett-Packard in 1964, he was engaged in the design of industrial and military cathode-ray tubes. He has been in the display devices group of the HP Colorado Springs Division where he was responsible for the design of the expansion mesh post-accelerator tube used in the HP Model 180A Oscilloscope.

Milt is a member of Tau Beta Pi, Eta Kappa Nu, and is a Senior Member of IEEE.

'Flying Clock' Comparisons Extended to East Europe, Africa and Australia

Using portable atomic clocks, HP teams recently brought precise time and frequency information to 18 countries.

By LaThare N. Bodily and Ronald C. Hyatt

ONE OF THE MOST ACCURATE MEASUREMENTS of which the measuring art is presently capable is the measurement of frequency or of its inverse, time interval. Such measurements can be made with an accuracy of a few parts in 10^{12} (and with even higher resolution — about 1 part in 10^{13}).

Since there is virtually no way to distribute high-accuracy frequencies over a distance without loss of precision and purity, members of the world scientific community working in the high-accuracy time and frequency field must necessarily generate their standard frequency locally. This brings about a need to intercompare standard frequencies. Similarly, laboratories involved with accurate timekeeping have a need to correlate their locally-kept time with each other and with the agencies that are officially charged with establishing standard time.

One of the most satisfactory methods for intercomparing frequency and time between distant places is to carry an accurate clock, usually by airplane, between the various places where frequency and time are of interest. Engineers from the HP Frequency and Time Division have recently conducted such a 'flying clock' experiment

Table I

Summary of HP Flying Clock Experiments

Date	Description
April, 1964	Time correlated between U.S. and Switzerland to about 1 microsecond. RF propagation time established within about 200 microseconds. Two clocks (#1 and 2) operated within a few parts in 10^{12} of one another and within a few parts in 10^{12} of "long beam" cesium standards at Neuchatel, Switzerland and NBS at Boulder, Colorado.
Feb./Mar., 1965	Time (or frequency) correlated between 21 places in 11 countries to within 1 microsecond. One clock (#3) accumulated less than 6 microseconds time difference and the other (#4) less than 1 microsecond in 23 days (compared against NBS UA).
May/June, 1966	Time (or frequency) correlated within about 0.1 microsecond between 25 places in 12 countries. Two clocks (#8 and 9) agreed with each other within 1 microsecond after 31 days with an average frequency difference of less than 3.6 parts in 10^{13}.
Sept./Oct., 1967	Time (or frequency) correlated between 53 places in 18 countries to about 0.1 microsecond. Two clocks (#51 and 52) exhibited time differentials of 1.7 and 3.5 microseconds over 41 days (compared to HP house standard), corresponding to average frequency differences of 5×10^{-13} and 10×10^{-13}, respectively.

which carried precise frequency and time information to 18 countries. This was the fourth and by far the most extensive experiment of its type conducted by the HP Frequency and Time Division.

The experiment extended over 41 days and the clocks jointly covered a total of some 100,000 kilometers (see map). Two HP clocks and three HP teams participated.* By comparing with the HP house standard at the beginning and end of the trip, the time differences of these clocks at the end of the 41 days were found to be only 1.7 and 3.5 microseconds. This corresponds to offsets of only 5 and 10 parts in 10^{13} in the frequency standards that actuate the clocks. The time correlations on the trip were made to a net accuracy of about 0.1 microsecond.

* At the HP office in Geneva, a third clock was synchronized with the two flying clocks and then carried to two facilities in Europe.

Fig. 1. *Atomic-controlled cesium beam frequency standard and clock assembly, complete with standby battery power supply, as used in 1967 Hewlett-Packard flying clock time comparisons.*

Table II

Stations Visited by 1967 Flying Clocks

Country	Comparison Made	Facility	Location
① Australia	T	① Stadan Tracking Station	Canberra
	F	② Australian Army Design	Melbourne
	F	③ Commonwealth Scientific and Industrial Research Organization	Chippendale
	T-F	④ MSFN Tracking Station	Canberra
	T-F	⑤ Mt. Stromlo Observatory	Canberra
	T-F	⑥ Postmaster General Research Lab.	Melbourne
② Belgium	T	⑦ Universite Libre de Bruxelles	Brussels
③ Canada	T-F	⑧ Dominion Observatory	Ottawa
	T-F	⑨ National Research Council	Ottawa
④ Czechoslovakia	T-F	⑩ Institute of Radio Engineering and Electronics, Czech. Academy of Sciences	Prague
	T	⑪ Astrom. Institute, Czech. Academy of Sciences	Prague
	T	⑫ Geodetic Observatory, Czech. Academy of Sciences	Pecny
	T	⑬ OMA Standard Broadcast Station	Liblice
⑤ Denmark	T	⑭ Laboratoriet Flyvestation Vaerlose	Vaerlose
⑥ England	T-F	⑮ National Physical Laboratory	Teddington
	T-F	⑯ Royal Greenwich Observatory	Hailsham
	T-F	⑰ Stadan Tracking Station	Winkfield
⑦ France	T	⑱ Centre National d'Etudes des Telecommunications	Bagneux
	T-F	⑲ Paris Observatory (BIH)	Paris
	F	⑳ Centre Technique de L'Industrie Horlogere	Besancon Ⓐ
	T	㉑ Observatoire de Besancon	Besancon Ⓐ
⑧ Germany	T	㉒ Deutsches Hydrographisches Institut	Hamburg
	T-F	㉓ Physikalisch-Technische Bundesanstalt	Braunschweig
⑨ Italy	T-F	㉔ Istituto Superiore Poste e Telecomunicazioni	Rome
	T-F	㉕ Centro Microonde	Florence
	T-F	㉖ Istituto Electtrotecnico Nazionale	Torino
	T-F	㉗ Milano Istituto Astronomica	Milano
⑩ Japan	T-F	㉘ Radio Research Laboratories	Koganei
⑪ Norway	T-F	㉙ Norwegian Air Force	Kjeller
⑫ Rumania	T-F	㉚ Observatoire de Bucarest	Bucharest
⑬ South Africa	T-F	㉛ Republic Observatory	Johannesburg
	T-F	㉜ Stadan Tracking Station	Johannesburg
	T-F	㉝ JPL Tracking Station	Johannesburg
⑭ Sweden	T-F	㉞ Forsvarets Forskningsanstalt	Stockholm
⑮ Switzerland	T-F	㉟ Hewlett-Packard S.A.	Geneva
	F	㊱ Laboratoire Suisse de Recherches Horlogeres	Neuchatel
	T	㊲ Observatoire de Neuchatel	Neuchatel
	F	㊳ Ebauches S.A.	Neuchatel
	T	㊴ HBG Standard Broadcast Station	Prangins
⑯ Turkey	T-F	㊵ Kandilli Observatory	Istanbul
⑰ Yugoslavia	T-F	㊶ Astronomska Observatorija	Belgrade
⑱ U.S.A.	T-F	㊷ Hewlett-Packard Company	Palo Alto
	T-F	㊸ National Bureau of Standards	Boulder, Colo.
	T	㊹ WWV Standard Broadcast Station	Ft. Collins, Colo.
	T	㊺ WWVB/L Standard Broadcast Stations	Ft. Collins, Colo.
	T-F	㊻ Goddard Space Flight Center	Greenbelt, Md.
	T-F	㊼ U. S. Naval Observatory	Washington, D.C.
	F	㊽ U. S. Naval Research Labs	Washington, D.C.
	F	㊾ Harvard University	Cambridge, Mass.
	F	㊿ Hewlett-Packard Company	Beverly, Mass.
	T-F	51 WWVH, Standard Broadcast Station	Maui, Hawaii
	T-F	52 U.S.N. Astronautics Group, Detachment "C"	Wahiawa, Oahu, Hawaii
	T-F	53 Omega Station	Haiku, Oahu, Hawaii

T Denotes Time Comparison.　　F Denotes Frequency Comparison.　　Ⓐ Visit made by FC #7 from HPSA office.

Considering the numerous on-loadings, off-loadings, plane rides (27 for one clock), car rides, hand portages, and cart portages, it can certainly be stated that the clocks proved themselves to be rugged as well as one of the world's highest-precision devices.

By means of the trip, time and/or frequency were correlated at 53 installations. For the first time visits were made into eastern Europe where, in fact, the team visiting Prague was introduced to a new technique for clock synchronization, as described later. Comparisons were also made at five NASA tracking stations.

In addition to visiting the U.S.A., Canada, Europe and eastern Europe, teams also visited installations on the Asian continent near Istanbul, as well as installations in and near Johannesburg on the African continent, and in and near Sydney, Canberra, and Melbourne in Australia.

14

Portable Clocks

The clocks were of a new generation which included advances developed from past experience and by state-of-the-art progress. The new clocks were smaller than those used previously (Fig. 1) and lighter by 70 pounds. Consequently, it was simple for them to be transported in the regular passenger seats of commercial airplanes.

The lighter weight and smaller size came about because the new clocks are an integrated combination of a count-accumulating system and a cesium-beam frequency standard. In past experiments the clock mechanism and frequency standard were not so integrated, although they were connected to achieve the same end result. As in the past, the clocks were combined with a portable battery and multi-voltage power converter so that they could operate either without external power or from a variety of ac and dc power sources.

Table III

Time Closures

The flying clocks (FC51 and FC52 in the data below) made a number of "time closures" with recognized time-keeping stations. This table shows five of the stations involved, the accumulated time differences between the flying clocks and the station clocks, and the average frequency difference between the frequency standards actuating the clocks for the interval of the closure. "FC51" and "FC52" in the table are the flying clocks.

Goddard Space Flight Center, Greenbelt, Md.	18 Oct.–12 Sept. Δ [FC52–GSFC*]	= 1.1 μsec
	Avg. Freq Difference = +0.4 × 10⁻¹² for 36 days	FC52 High
USNO, Wash., D.C.	18 Oct.–12 Sept. Δ [FC52 — USNO M.C.]	= −7.1 μsec
	Avg Freq Difference = −2.3 × 10⁻¹² for 36.3 days	FC52 Low
NBS, Boulder, Colorado	19 Oct.–11 Sept. Δ [FC52–NBS 8*]	= −3.3 μsec
	Avg Freq Difference = −1.0 × 10⁻¹² for 38.3 days	FC52 Low
WWV, Ft. Collins, Colo.	20 Oct.–11 Sept. Δ [FC52–WWV*]	= −0.8 μsec
	Avg Freq Difference = −0.2 × 10⁻¹² for 39.2 days	FC52 Low
Hewlett-Packard, Palo Alto	21 Oct–10 Sept. Δ [FC52–hp(A3)]	= −1.7 μsec
	Avg Freq Difference = −0.5 × 10⁻¹² for 40.3 days	FC52 Low
Hewlett-Packard, Palo Alto	22 Oct.–10 Sept. Δ [FC①51–hp(A3)]	= −3.5 μsec
	Avg Freq Difference = 1.0 × 10⁻¹² for 41 days	FC51 Low
Hewlett-Packard, Palo Alto	22 Oct.–10 Sept. Δ [FC51–FC52]	= −1.8 μsec
	Avg Freq Difference = 0.5 × 10⁻¹² for 41 days	FC51 Low

* Clocks advanced 200 μsecs 20 Sept. 1967.
① FC51 time corrected to account for interruption of normal operation 16 Sept.

Table IV

Time Scale Comparisons

This table shows the difference between several locally-maintained time scales and the NBS UA time scale for two checks made 16 months apart via the flying clocks. The small time changes show that the various time scales are within about 2 parts in 10^{12} of one another.

| | 1966 | | 1967 | | |
Facility	Date	Time Diff. μsec	Date	Time Diff. μsec	Change μsec
Radio Research Lab	18 May	1,474	16 Oct.	1,400	−74
Nat'l Research Council	19 May	200,489	18 Sept.	200,557	+68
USN Observatory	18 May	79	11 Sept.	165	+86
Neuchatel (TUA) Observatory	22 May	2,405	23 Sept.	2,468	+63
Dom'n Observatory	20 May	1	17 Sept.	54	+53
Physikalisch-Technische Bundesanstalt	3 June	433①	26 Sept.	489	+56
Royal Greenwich Observatory	3 June	59	4 Oct.	154	+95

① 1966 time difference value corrected for known time scale frequency offset existing from 3 June to 30 December, 1966.

The new clocks also incorporated a digital type of frequency divider rather than the regenerative type used in the first two experiments. This new circuitry was first tried in last year's experiment with good success and has been designed into the new time standard.

Initial Adjustments

Readers working in the atomic oscillator field are often interested in knowing the method used to establish the operating frequency of the cesium standards used in the clocks. This question arises because, although the cesium standards are primary standards whose frequency depends on a fundamental natural phenomenon, one of the initial adjustments can affect this frequency. This adjustment is the strength of the magnetic field ('C' field) that surrounds the cesium beam. The 'C' field has a nominal value but can be changed slightly to affect the transition frequency of the cesium atoms.

In the experiment both clocks were initially phase-compared with the HP house frequency standard (HPA3), one of the world's most accurate standards. One clock had no offset from this standard, while the 'C' field of the second clock was specifically adjusted to bring the frequency into closer agreement with the house standard (within the limits of measurement resolution, about 1–2 parts in 10^{13}).

At the end of the 41-day trip, the two flying clocks were found to have operated within five parts in 10^{13} of one another's average frequency. Compared to the HP

Table V

Frequency Comparisons with Atomic Standards

This table presents a listing of the frequency comparisons between the visiting flying clock and the atomic frequency standard(s) at the station visited. A note indicates how the measurement was made. "FC51" and "FC52" in the table refer to the flying clock.

Date	Local Std.	Type (Cesium except as noted — length denotes interaction length)	Comparison
12 Sept.	NBS III (U.S.) Boulder, Colorado	366 cm Lab Type	−299.994 ± .002 × 10⁻¹⁰ 175 ea 393 sec. samples FC51 High
11 Sept.			−300.012 ± .027 × 10⁻¹⁰ 9 ea 393 sec samples FC52 Low
20 Oct.			−299.996 ± .003 × 10⁻¹⁰ 135 ea 393 sec samples FC52 High
12 Sept.	USNO Washington, D.C.	12.4 cm commercial	−0.7 ± 0.3 × 10⁻¹² 11.5 Hr Phase Comp FC52 Low
20 Sept.			−1.6 ± 0.2 × 10⁻¹² 17.8 Hr Phase Comp FC51 Low
19 Oct.			−5.2 ± 0.4 × 10⁻¹² 16.6 Hr Phase Comp FC52 Low
14 Sept.	HPSA #8 (Switzerland)	12.4 cm commercial	+0.4 ± 0.2 × 10⁻¹² 21 Hr Phase Comp FC52 High
22 Sept.			−0.2 ± 0.2 × 10⁻¹² 22.5 Hr Phase Comp FC51 Low
3 Oct.			−0.8 ± 0.2 × 10⁻¹² 85 Hr Phase Comp FC51 Low
17 Oct.			−2.0 ± 0.2 × 10⁻¹² 23 Hr Phase Comp FC52 Low
18 Sept.	Dominion Observatory (Canada)	12.4 cm commercial	+0.4 ± 0.5 × 10⁻¹² 14.5 Hr Phase Comp FC51 High
19 Sept.	NRC (Canada)	200 cm Lab Type	−299.995 ± .013 × 10⁻¹⁰ 200 - 38 sec samples FC51 High
18 Sept.	FOA (Sweden)	Std #1 12.4 cm commercial	+0.7 ± 0.2 × 10⁻¹² 36 Hr Phase Comp FC52 High
		Std #2 12.4 cm commercial	+0.2 ± 0.2 × 10⁻¹² 36 Hr Phase Comp FC52 High
19 Sept.	NAF (Norway)	12.4 cm commercial	−299.946 ± .006 × 10⁻¹⁰ 18.6 Hr Phase Comp FC52 High
20 Sept.	ISPT (Italy)	Rubidium	+3.0 × 10⁻¹² 1.5 Hr Phase Comp FC52 High
28 Sept.	MIA (Italy)	Rubidium	−1.74 × 10⁻¹⁰ 0.6 Hr Phase Comp FC52 Low
23 Sept.	Ebauches, S.A. (Switzerland)	25 cm commercial	+0.6 ± 0.2 × 10⁻¹² 15 Hr Phase Comp FC51 Low
26 Sept.	PTB (Germany)	88 cm commercial	−299.998 × 10⁻¹⁰ 16 Hr Phase Comparison FC51 High
27 Sept.		12.4 cm commercial	−300.006 × 10⁻¹⁰ 13 Hr Phase Comp FC51 Low
2 Oct.	NPL (England)	12.4 cm commercial	−300.039 ± .008 × 10⁻¹⁰ 24 Hr Phase Comp FC52 Low
4 Oct.	RGO (England)	12.4 cm commercial	−300.000 ± .004 × 10⁻¹⁰ 4 Hr Phase Comp Via FC52
6 Oct.	Paris Obs. (France)	25 cm commercial	−299.862 × 10⁻¹⁰⑤ 100 ea 100 sec samples FC52 High

Date	Local Std.	Type	Comparison
6 Oct.	JPL Tracking Station (So. Africa)	Rubidium	+4.88 × 10⁻¹⁰ 1 Hr Phase Comp FC51 High
9 Oct.	Rep. Obs. (So. Africa)	12.4 cm commercial	−299.943 × 10⁻¹⁰ 62 Hr Phase Comp FC51 High
10 Oct.	CSIRO (Australia)	12.4 cm commercial	−300.039 ± .002 × 10⁻¹⁰ 22 Hr Phase Comp FC51 Low
11 Oct.	Mt. Stromlo Obs. (Australia)	12.4 cm commercial	−2.3 ± 0.2 × 10⁻¹² 14 Hr Phase Comp FC51 Low
12 Oct.	MSFN Tracking Sta. (Australia)	Rubidium	−2.54 × 10⁻¹¹ 1 Hr Phase Comp FC51 Low
12 Oct.	Aust. Army Design (Australia)	12.4 cm commercial	−299.978 × 10⁻¹⁰ 4 Hr Phase Comp FC51 High
14 Oct.	PMG (Australia)	12.4 cm commercial	−299.975 × 10⁻¹⁰ 17.7 Hr Phase Comp FC51 High
19 Oct.	RRL (Japan)	Std #1 12.4 cm commercial	+7.2 × 10⁻¹² 25 Hr Phase Comp FC51 High
		Std #2 12.4 cm commercial	−0.6 × 10⁻¹² 57 Hr Phase Comp FC51 Low
19 Oct.	Mizusawa⑥ (Japan)	12.4 cm commercial	−0.4 × 10⁻¹² 28 Hr Phase Comp FC51 Low
20 Oct.	USN Astron. (Hawaii)	12.4 cm commercial	−3.4 ± 0.3 × 10⁻¹² 20 Hr Phase Comp FC51 Low
21 Oct.	Omega (Hawaii)	12.4 cm commercial	−0.1 ± 0.3 × 10⁻¹² 12.5 Hr Phase Comp FC51 Low

NOTES

① Flying Clocks operated on UTC Time Scale −300.00 × 10⁻¹⁰.

② Frequency comparisons given as offset from A1 when compared against standards with nominal frequency other than −300.00 × 10⁻¹⁰.

③ Fractional frequency difference between UTC Clocks is computed as: Freq. Dev. $= (f_t − f_L)/f_n$ where f_t, f_L and f_n are frequencies of traveling clock, local clock and nominal frequency respectively. Freq. deviation is positive if f_t is higher in frequency than f_L and negative if f_t is lower than f_L.

④ Frequency comparisons are reported as measured without correction for ambient magnetic field and temperature effects on the flying clocks.

⑤ Frequency offset due to observatory cesium beam electronic circuitry.

⑥ Measured at RRL facility.

house standard, one clock operated at an average of within five parts in 10^{13}, the other within ten parts in 10^{13} of the average house standard frequency.

Cesium and Hydrogen Standards

The places visited this year are shown in Table II and the resulting measurements and data are in Tables II–VI. As in past experiments, intercomparisons were also made with several of the world's long-beam cesium standards which represent the first generation of cesium standards. The present portable standards represent the most recent generation.

Comparisons were also made with most of the world's independently-constructed hydrogen maser frequency standards. These comparisons require further reduction of the comparison data; this is now being done by the participants and will be published separately.

Flying Clocks

The experiment described on p. 12 is the fourth such 'flying clock' experiment conducted by the Hewlett-Packard Company. The objects of these experiments have been to improve the body of knowledge about the overall accuracy of the world family of atomic frequency standards and to achieve a more accurate correlation and synchronization of time throughout the world.

The flying clock method of intercomparing frequency standards has clearly shown itself to be a principal method of accomplishing these aims. In essence, the method consists of transporting an atomic clock from place to place, usually by air. Since the clock derives its accuracy from an internal atomic frequency standard, presently one of the most accurate devices in existence, it is also possible to compare this internal standard with other standards — and through this process to compare all standards with one another.

The frequency of the standard in the portable clock, as well as the time kept by the clock, is established at the beginning of the trip by direct comparison with national standards at the National Bureau of Standards and U.S. Naval Observatory. After the trip the loop is closed by re-comparing the portable clock with these same standards so that the slight changes that inevitably occur can be referred back as a tolerance on the previous measurements.
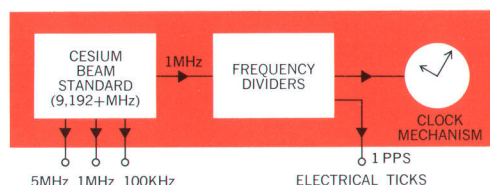
The precision achieved in relating the various standards to one another with a portable clock is very high indeed. The results of the past HP experiments show, for example, that the standards participating in the experiment were compared to a precision of parts in 10^{13}. It is notable that such precision is probably several hundred to one thousand times better than that with which any other physical quantity can be measured. In those same experiments the time of day at each participating station was correlated to within about 0.1 microsecond — typically at least several orders of magnitude better than previous radio wave measurements.

The factor that has enabled flying clocks to evolve as the most precise method for intercomparing frequency and time at a distance is the extreme accuracy presently achieved in the atomic standard which actuates the clocks. Measurements on a large number of HP Cesium Beam Frequency Standards have, for example, shown the accuracy of the full group to be within about ± 5 parts in 10^{12} of the mean. These standards are those used in the flying clocks, and their accuracy has permitted the measurement precision noted above in intercomparing the world's best-known atomic standards.

The cesium beam frequency standard is itself a primary standard since it derives its accuracy from a constant of nature which is presumed invariant. The con-

stant referred to is a transition in the cesium 133 atom between two particular hyperfine energy levels. The frequency of this transition has been defined by the Thirteenth General Conference of Weights and Measures as occurring at 9, 192, 631, 770 hertz (cps). As well as defining a frequency, this definition also defines an 'atomic second' and consequently an 'atomic time' scale which is now used in much accurate work. This scale is considerably more uniform than the rotation of the earth which is the basis for other time scales.

The clocks used in this most recent 1967 experiment operate from a cesium standard of latest design (HP Model 5061A) which contains circuitry permitting either atomic time or UTC (Coordinated Universal Time) to be kept. UTC is an approximation to UT2 which is based on the rotation of the earth and determines the length of the second (and frequency) as broadcast by NBS stations WWV, WWVH, and WWVL, and by stations coordinated by the U.S. Naval Observatory. The length of the second in the UTC scale is set yearly by the Bureau International de l'Heure in Paris and is presently longer than the atomic scale by 300 parts in 10^{10}. Frequencies based on the UTC scale are thus lower than those of the atomic scale by the same amount. In the new 5061A Standard the time scale can be changed merely by setting four thumbwheels and a switch, and by adjusting the "C" magnetic field.

Clocks' basic circuit arrangement.

The basic circuit arrangement of the clocks appears in the diagram. An accurate frequency standard (the atomic standard) is the heart of the equipment and produces an accurate frequency which is integrated by a clock to measure the passage of time. As a by-product of the circuitry, electrical 'ticks' are produced which are useful in precision comparisons between the clock and other systems. Also produced are various other frequencies which are used as standard frequencies and in the intercomparison of various accurate frequencies. These intercomparisons are generally made by comparing the phases of the two frequencies for intervals of several hours.

Table VI

*Time differences measured between local station clocks and
on arbitrarily-selected reference (HP house standard).
These measurements were made by the visiting flying clocks
and have been adjusted for known differences between the
flying clock and the HP house standard (HPA3).*

NOTE: In this table time differences are reported in the form: *Clock A − Clock B = D* where D is positive
if reading A is greater than reading B (Clock A tick occurs first). Reading A in the table is always that of
the clock at the visited facility; Clock B is always the flying clock. This arrangement has been followed to
be consistent with last year's reported time differences and with the recommendations for reporting such
data made by the Commission de l'Heure of the Int'l Astronomical Union (August '67).

Date	Time (UT)	Facility			Comparison (μsec)
11 Sept.	14^H11^M	NBS, Boulder, Colo.	NBS(8) — hp	=	−165.8
11 Sept.	14^H40^M	WWV, Ft. Collins, Colo.	WWV① — hp	=	−163.5
11 Sept.	$15^H19^M00^S$	WWVB, Ft. Collins, Colo.	WWVB①* — hp	=	962,120.7
11 Sept.	15^H20^M	WWVL, Ft. Collins, Colo.	WWVL① — hp	=	−147.2
11 Sept.	$17^H22^M45^S$	NBS, Boulder, Colo.	NBS(7)* — hp	=	5,962,343.0
11 Sept.	23^H53^M	USNO, Washington, D.C.	USNO(M.C.) — hp	=	−0.5
12 Sept.	$00^H06^M30^S$	USNO, Washington, D.C.	USNO(220)* — hp	=	5,952,141.9
12 Sept.	14^H50^M	GSFC, Greenbelt, Md.	GSFC — hp	=	−205.7
13 Sept.	09^H18^M	HPSA, Geneva, Switzerland	HPSA(8) — hp	=	−19.0
14 Sept.	16^H09^M	Danish Air Force, Denmark	RDAF — hp	=	−2,587.7
15 Sept.	14^H20^M	Swedish Nat'l. Def. Lab., Sweden	FOA② — hp	=	−312.8
17 Sept.	22^H34^M	Dominion Obs., Ottawa	DO③ — hp	=	−112.0
18 Sept.	13^H00^M	Norwegian Air Force, Norway	NAF* — hp	=	−12,536.3
18 Sept.	16^H45^M	Nat'l. Research Council, Ottawa	NRC — hp	=	200,391.5
20 Sept.	08^H57^M	Ist. Sup. Poste e Tele., Rome	ISPT — hp	=	29.1
21 Sept.	08^H03^M	Centro Microonde, Florence	CM — hp	=	−1,910.0
22 Sept.	08^H35^M	Ist. Elecct. Nazionale, Torino	IEN① — hp	=	−6.7
23 Sept.	07^H30^M	Obs. Neuchatel, Neuchatel	HBN — hp	=	1,011.6
23 Sept.	10^H08^M	HBG, Prangins	HBG① — hp	=	−179.4
23 Sept.	13^H15^M	HPSA, Geneva	HPSA(8) — hp	=	−19.8
25 Sept.	09^H18^M	Deut. Hydro Inst., Hamburg	DHI⑤ — hp	=	−606.1
25 Sept.	09^H51^M	Milano Ist. Obs., Milano	M.I.O. — hp	=	−1,268.2
25 Sept.	17^H47^M	HPSA, Geneva	HPSA(8) — hp	=	−19.8
26 Sept.	07^H30^M	PTB, Braunschweig	PTB(TUA) — hp	=	323.4
			PTB*(A1) — hp	=	5,955,236.4
			PTB⑥(SAI) — hp	=	477.0
28 Sept.	09^H52^M	Inst. Radio Engr., Prague	IRE(BO) — hp	=	−1,083.4
			IRE(CO) — hp	=	321.4
28 Sept.	13^H45^M	OMA — Std. Broadcast Sta., Liblice	OMA① — hp	=	−1,051.2
28 Sept.	15^H15^M	Geodetic Obs., Pecny	GO (Clock A) — hp	=	−1,196.8
29 Sept.	07^H55^M	Inst. Radio Engr., Prague	IRE(CO) — hp	=	316.5
			IRE(BO) — hp	=	1,084.5
29 Sept.	08^H30^M	Geodatisches Institut of German Academy of Sciences, Potsdam	GI⑦(HU) — hp	=	2,500.
29 Sept.	07^H44^M	Belgrade Obs., Belgrade	Bel. Obs. — hp	=	−92,320.5
29 Sept.	09^H58^M	Astronomical Inst., Prague	AI(HI) — hp	=	313.2
30 Sept.	17^H40^M	HPSA, Geneva	HPSA(8) — hp	=	−19.6
2 Oct.	09^H54^M	Stadan Tracking Station, Winkfield, England	Stadan⑧ — hp	=	−527.
2 Oct.	$14^H41^M30^S$	Nat. Physical Lab., Teddington, England	NPL(A1)* — hp	=	407,174.1
2 Oct.	14^H47^M	Nat. Physical Lab., Teddington, England	NPL(S40) — hp	=	−311,981.4
4 Oct.	$08^H32^M00^S$	Kandilli Observatory, Istanbul	KO(K₂)* — hp	=	22,434.3
4 Oct.	10^H38^M	Royal Greenwich Obs., Hailsham	RGO(MC)⑨ — hp	=	−12.0
5 Oct.	15^H55^M	Paris Observatory, Paris	PO(HO)⑩ — hp	=	−305.1
	$00^H00^M00^S$		A3* — PO(HO)	=	5,977,655
6 Oct.	11^H48^M	Stadan Tracking Station, Johannesburg	MT(HE101)⑪ — hp	=	−567.
6 Oct.	13^H30^M	Observatoire de Besancon, Besancon	Ob. Besancon(Q7)⑫ — hp	=	−125,386.0
6 Oct.	13^H59^M	JPL Tracking Station, Johannesburg	DSIF 51 — hp	=	−1,651.7
6 Oct.	17^H00^M	Republic Observatory, Johannesburg	RO — hp	=	−773.5
9 Oct.	13^H20^M	CNET, Bagneux, France	CNET — hp	=	−431.
11 Oct.	07^H46^M	Mt. Stromlo Observatory, Canberra	MSO — hp	=	1,061.

Date	Time (UT)	Facility		Comparison (μsec)
11 Oct.	14^{H}25^M	Obs. Bucarest, Bucarest	Obs. Buc. (R1) — hp =	−6,254.7
12 Oct.	01^{H}10^M	MSFN Tracking Station, Canberra	MSFN — hp =	−447.5
12 Oct.	03^{H}35^M	Stadan Tracking Station, Canberra	Stadan[7] — hp =	2,368.
13 Oct.	05^{H}20^M	PMG, Melbourne	PMG — hp =	729.9
13 Oct.	15^{H}57^M	Univ. Brussels, Brussels	UB — hp =	2,905.2
16 Oct.	02^{H}00^M	Radio Research Lab., Koganei	RRL — hp =	1,235.7
16 Oct.	12^{H}25^M	HPSA, Geneva	HPSA(8)[14] — hp =	−0.1
18 Oct.	14^{H}19^M	GSFC, Greenbelt, Md.	GSFC[15] — hp =	−8.4
18 Oct.	19^{H}46^M	USNO, Washington, D.C.	USNO — hp =	5.0
18 Oct.	20^{H}07^{M}30^S	USNO, Washington, D.C.	USNO(220)* — hp =	6,047,608.9
19 Oct.	21^{H}35^M	NBS, Boulder, Colo.	NBS(8)[15] — hp =	35.8
19 Oct.	21^{H}37^{M}30^S	NBS, Boulder, Colo.	NBS(7*) — hp =	6,061,299.5
19 Oct.	23^{H}12^M	USN Astro Group, Oahu, Hawaii	USNA — hp =	10.7
20 Oct.	18^{H}54^M	WWV, Ft. Collins, Colo.	WWV[1][16] — hp =	35.5
20 Oct.	19^{H}28^M	WWVL, Ft. Collins, Colo.	WWVL[1][16] — hp =	52.9
20 Oct.	19^{H}32^{M}00^S	WWVB, Ft. Collins, Colo.	WWVB[1][15]* — hp =	63,664.8
20 Oct.	23^{H}10^M	WWVH, Maui, Hawaii	WWVH[1] — hp =	37.9
21 Oct.	04^{H}20^M	Omega Station, Oahu, Hawaii	Omega — hp =	12.8

* Denotes Atomic Time.

[1] Transmitter station clock which controls tick to transmitter.

[2] FOA clock reset 18 Sept. 0740 to agree with USNO M.C.

[3] Coincides with CHU emission time, ±0.1 msec.

[4] Coincides with IBF emission time.

[5] Coincides with DAM emission time, ±0.1 msec.

[6] Stepped atomic time — coincides with DCF 77 emission time.

[7] Check at Inst. Radio Eng. and Electronics of Czech. Acad. Sciences, Prague, via TV method described in Vol. IM-16, No. 3, Sept. 1967, pp 247–254, IEEE Trans. on Inst. and Meas. Clock HU controls emission of time signal of DIZ.

[8] Value stated has been adjusted by 26.12 msec to account for calculated RF propagation time of comparison signal from standards station.

[9] RGO(MC) — MSF$_{60kHz}$ = 400 μsec (MSF standard broadcast station emission as received at Royal Greenwich Observatory on 5 Oct. at 14^{H}36^M with estimated propagation delay removed).

[10] Coincides with FTA 91, FTH 42, FTK 77, FTN 87 emission times, ±50 μsecs.

[11] Value stated has been adjusted by 53.67 msec to account for calculated RF propagation time of comparison signal from standards station.

[12] Measurement made with FC 7 from HPSA office.

[13] Value stated has been adjusted by 30.10 msec to account for calculated RF propagation time of comparison signal from standards station.

[14] HPSA reset to agree approximately with USNO M.C. on 16 Oct.

[15] Ticks advanced 200 μsec 20 Sept. 1967.

Prague - Potsdam Synchronization

The visit to the Czechoslovak Academy of Sciences at Prague represented the first time the flying clocks have traveled to eastern Europe. This visit was also marked by a novel method which was in use in Prague for synchronizing a distant clock. The method was employed by the Czech scientists during the Prague synchronization to simultaneously synchronize a clock in Potsdam, Germany, some 300 kilometers distant.

In essence, the method requires both places to measure simultaneously the time interval between their clock pulses and a previously-designated sync pulse from a TV station. The method is not necessarily limited to the distance at which the two places can receive the same TV station, since relay links can be used for the transmission if desired. The method requires that a suitable propagation-time correction be applied, but this is readily done. Further details and other variations of the method are described in a recent paper.*

* Jiri Tolman, Vladimir Ptacek, Antonin Soucek, and Rudolf Stecher, 'Microsecond Clock Comparison by Means of TV Synchronizing Pulses,' IEEE Transactions on Instrumentation and Measurement, Vol. IM-16, No. 3, September, 1967.

Clock Recomparison

In an experiment of this duration and complexity it is, to say the least, statistically improbable that no untoward event will occur. In other years the experiments have overcome such unforeseen events as the power being switched off while the clocks were stored overnight in a locked hotel room and again by a defect in a monitoring circuit external to the clocks. This year one clock lost internal phase lock due to a foreign particle in a waveguide. Fortunately, this occurred while the clock was still in the U.S. (in Boston) in an early stage of the trip. The clock was not stopped but the loss of phase lock rendered its reading uncertain. The clock was repaired at the HP laboratory in nearby Beverly, Massachusetts, and then taken to Ottawa, Canada. After making a comparison there, the clock was returned to the U.S. Naval Observatory in Washington, D.C., for recomparison. At this time it was found that the clock reading differed by only one microsecond from its earlier comparison at USNO. This difference has been applied to the comparisons made after the interruption.

NBS Time Advance

The data concerning time closures in this year's experiment are corrected to account for an adjustment made in the UTC clock at the U.S. National Bureau of Standards. For some time the clocks at the U.S. Naval Observatory and the Bureau of Standards have exhibited a relative difference of about 1 part in 10^{12}. To bring these clocks into even closer synchronization, the NBS clock, through a previously-scheduled plan, was advanced 200 microseconds on September 20, midway between the visits made to the Bureau of Standards during the visit. Hence, the affected data published here have been corrected for this adjustment and for the similar adjustments made on the same date by Station WWV and by the Goddard Space Flight Center.

Relativistic Effects

After the publication of past flying clock articles in the Hewlett-Packard Journal, many readers have inquired for the information about relativistic effects on such measurements which involve clocks in motion.

The effects must be considered from the viewpoint of general relativity since relative motion, rotation and gravitation are all involved. At the altitudes and velocities of present-day commercial airliners, the effects are fairly small and yield the following approximate results.

A flying clock moving at constant velocity, v, and constant altitude, h, indicates an elapsed time, T_{fc}, different from that of a stationary clock, T_o, on the ground by a fractional amount

$$\frac{T_{fc} - T_o}{T_o} \approx \frac{gh}{C^2} - \frac{v^2}{2C^2}$$

where g is the acceleration of gravity (which includes the effect of rotation of the earth) and c is the velocity of light. In this approximation the gravitational and motional effects may be separated. The first term is the gravitational shift which is 'blue' since the flying clock is farther from the earth than the stationary clock. The second term is the 'time dilation' of special relativity caused by the relative velocity.

Consider a plane at an altitude of 35,000 feet with a ground speed of 650 miles per hour. For these conditions the 'blue' shift term is $+1.16 \times 10^{-12}$ and the time dilation term is -0.47×10^{-12}, or a total of $+0.69 \times 10^{-12}$. If the clock were in flight for eighty hours during the whole trip of one thousand hours (typical values), the 'blue' shift term gives an indicated elapsed time difference of about $+0.333$ microseconds and the time dilation term gives about -0.135 microseconds, on a total of $+0.198$ microseconds (the plus sign means the flying clock is ahead). This amount is somewhat smaller than that which may be expected from random errors and drifts in the clock rates.

Note that the relativistic effects are in opposite directions and that, for the conditions chosen, the gravitational term is dominant. At present they are not large enough to affect the measurements appreciably, but they are at the threshold. Significant improvement in either the clocks or aircraft could make relativistic corrections important.

There have also been questions as to whether clocks at sea level are not at the same rate independent of their location on the earth. Since the earth is approximately in hydrostatic equilibrium its surface may be viewed, in a coordinate system rotating with the earth, as a surface of constant gravitational potential (neglecting other bodies such as the sun and moon). Clocks located anywhere on such a surface do run at the same rate.

Acknowledgment

At every station the visiting teams found the staffs eager to cooperate in the experiments. This is sincerely appreciated as is the assistance of the many people in many places who worked so enthusiastically to make the experiments successful.

We also express our appreciation to Richard Baugh, Robert Kern, Felix Lazarus, and Anton Polsterer of the HP organization who took flying clocks to several stations, as well as to Dr. Leonard S. Cutler of the HP Beverly Laboratories who supplied the relativistic effect information. ⏚

Data in this report are stated in a format recommended by the Commission de l'Heure of the International Astronomical Union. In this format a positive algebraic sign assigned to the numerical difference between two frequencies or two clocks means the first-listed quantity (minuend) is higher, if a frequency, or earlier, if a clock. A negative sign means the first-listed quantity is lower or later, respectively.